Rotational motion of dimers of Janus particles

Arghya Majee*
Max-Planck-Institut für Intelligente Systeme, Heisenbergstr. 3, 70569 Stuttgart, Germany and
IV. Institut für Theoretische Physik, Universität Stuttgart, Pfaffenwaldring 57, 70569 Stuttgart, Germany

We theoretically study the motion of a rigid dimer of self-propelling Janus particles. In a simple kinetic approach without hydrodynamic interactions, the dimer moves on a helical trajectory and, at the same time, it rotates about its center of mass. Inclusion of the effects of mutual advection using superposition approximation does not alter the qualitative features of the motion but merely changes the parameters of the trajectory and the angular velocity.

arXiv:1703.09063v1 [cond-mat.soft] 27 Mar 2017

I. INTRODUCTION

Self-propelling Janus particles (JPs) have gained increasing attention in recent years from both theoreticians and experimentalists as they show a promising route towards the understanding of the motion of living microorganisms [1–4]. On the other hand, possible applications range from drug delivery to autonomous micromachines [5, 6]. Various types of microswimmers have been built in recent years which mainly rely on the nonuniform surface properties of the particle. Due to their asymmetric surface properties, these particles are able to generate their own gradient within an otherwise homogeneous medium and propel in this self-generated gradient. One particularly widely studied system in this context is chemical reaction driven self-propellers [7–10].

Of late, heating of half metal coated Janus particles has emerged as a possible way to achieve self-propulsion. The metal cap can absorb energy from laser irradiation [11, 12] or ac magnetic field [13] and convert it into heat. Asymmetric thermal response of the capped and uncapped hemispheres then drives the colloid via self-thermophoresis. For a rotationally symmetric single particle the resulting motion is linear initially; at longer times enhanced diffusion takes place due to rotational Brownian motion. However, a system of twin Janus particles with the one being tethered to the glass surface has been observed to rotate under laser irradiation [11]. Several other rotationally asymmetric systems have also been reported to show rotational movements. For example, circular motion of L-shaped asymmetric microswimmers on the substrate of a thin film and near channel boundaries has been reported [14]. Very recently, stable rotation was observed for a dimer system of chemically active Janus particles [15].

In this paper we consider a dimer of rigidly attached Janus particles, which is free to move and to rotate in three dimensions and applies best to the case of self-thermophoretic particles. Since usually the thermal conductivities of the solvent and the colloids are very close to each other, temperature field due to one particle is hardly affected by the presence of the neighbor particle. This is usually not the case for a dimer of catalytic Janus particles as in this case the solutes can not penetrate the other particle and the concentration gradient is affected by the presence of the second particle [16]. In our system, the orientation of the metal caps with respect to the dimer axis is kept arbitrary and each JP is treated in terms of a squirmer model where the local slip velocity at each particle surface is approximated by the first two Fourier components in an expansion in terms of the Legendre polynomial basis; see Eq. (11) below and the following discussion. As a first approach we use a simple model without hydrodynamic interactions. Then we retain mutual advection and forces in terms of a superposition approximation for the flow fields created by the two particles of the dimer.

II. DIMER MOTION

We consider the self-propulsion of a dimer, that is, of two Janus particles (squirmers) which are rigidly attached to each other. Their motion arises from an effective slip velocity $u_s(\theta)$, which is generated by a concentration or temperature gradient and depends only on the polar angle θ with respect to the symmetry axis. A single particle moves at a velocity

$$\mathbf{u}_0 = u_0\mathbf{n}, \tag{1}$$

where both its absolute value u_0 and direction $\mathbf{n}$ are determined by the weighted surface average of the slip velocity [17].

Two particles that are attached to each other, exert mutual forces and result in a more complex motion which depends on the relative orientation of the particles with respect to the dimer axis. To describe the motion of this system, it is convenient to separate the center-of-mass velocity $\mathbf{U}$ and the relative motion of the JPs. For a rigid dimer, the relative motion reduces to its angular velocity $\mathbf{\Omega}$.

We start with the simplest model which neglects advection. Then the center of mass motion is given by the mean value of the single-particle velocities,

$$\mathbf{U}_0 = \frac{\mathbf{u}_0 + \mathbf{u}_0'}{2}. \tag{2}$$

*Electronic address: majee@is.mpg.de

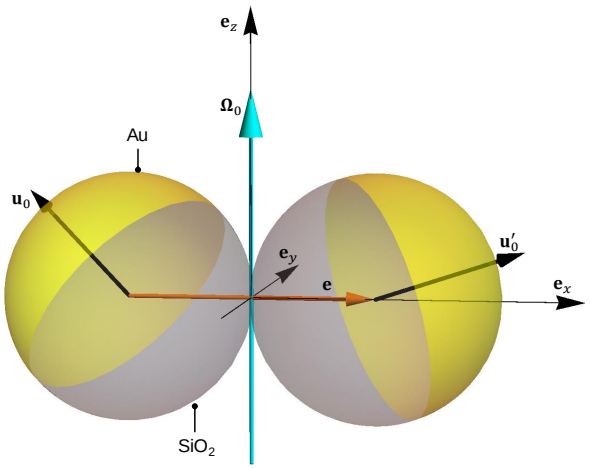

FIG. 1: Sketch of a dimer which consists of two Janus particles attached to each other in an arbitrary way. The co-ordinates are chosen in a way that the angular velocity vector $\boldsymbol{\Omega}_0$ is directed along z-axis, the dimer axis $\mathbf{e}$ lies along x-axis, the relative velocity $\mathbf{u}_0 - \mathbf{u}_0'$ is in the xy-plane.

The corresponding angular velocity,

$$\boldsymbol{\Omega}_0 = \frac{\mathbf{u}_0 - \mathbf{u}_0'}{2a} \times \mathbf{e}, \tag{3}$$

accounts for the orbital motion resulting from single-particle motion perpendicular to the dimer axis $\mathbf{e}$. As shown in Fig. 1, $\mathbf{e}$ points towards the primed particle.

In the absence of additional torques and forces, the absolute values of both linear and angular velocities are constant in time. The orientation of one or the other, or of both, may change depending on the three vectors $\mathbf{u}_0, \mathbf{u}_0', \mathbf{e}$. The linear velocity $\mathbf{U}_0$ also rotates at an equal rate

$$\frac{d}{dt}\mathbf{U}_0 = \boldsymbol{\Omega}_0 \times \mathbf{U}_0. \tag{4}$$

It turns out convenient to separate the velocity in two components $\mathbf{U}_0 = \mathbf{U}_0^{\parallel} + \mathbf{U}_0^{\perp}$ which are parallel and perpendicular to the angular velocity. Then the trajectory of the center of mass consists of a linear motion with velocity $\mathbf{U}_0^{\parallel}$, and a rotation in the plane perpendicular to $\boldsymbol{\Omega}_0$; the latter is characterized by the angular velocity Ω_0 and a circular trajectory of radius

$$R_0 = U_0^{\perp}/\Omega_0. \tag{5}$$

The dimer axis is always perpendicular to $\boldsymbol{\Omega}_0$ and thus obeys the equation of motion

$$\frac{d}{dt}\mathbf{e} = \boldsymbol{\Omega}_0 \times \mathbf{e}. \tag{6}$$

Since the angular velocity $\boldsymbol{\Omega}_0$ is perpendicular on $\mathbf{e}$, it is constant in time.

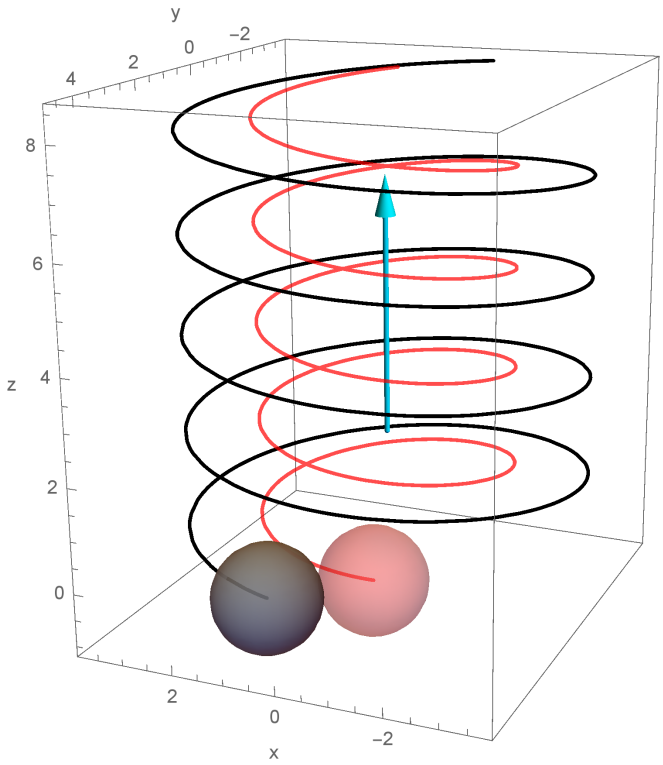

FIG. 2: Sample trajectory for the centers of the two particles forming the dimer. The arrow shows the direction of the angular velocity and the linear motion of the dimer. The particles rotate about the center of mass of the dimer at a rate similar to the rotation of the center of mass itself.

Thus the trajectories of the two JPs depend on the relative orientation of $\boldsymbol{\Omega}_0$ and $\mathbf{U}_0$ and consist of two contributions: The dimer shows translational motion at velocity $\mathbf{U}_0^{\parallel}$ along the vertical axis $\hat{\mathbf{z}}$ defined by $\boldsymbol{\Omega}_0 = \Omega_0\hat{\mathbf{z}}$. Both $\mathbf{U}_0^{\perp}$ and $\mathbf{e}$ rotate about this axis at the angular velocity Ω_0. The center of mass moves on a helical trajectory

$$\mathbf{R}_{\rm cm} = U_0^{\parallel} t\hat{\mathbf{z}} + R_0\hat{\varphi}(\Omega_0 t), \tag{7}$$

where $\hat{\varphi}$ is the local basis vector corresponding to the azimuthal angle φ. At the same time, the dimer axis $\mathbf{e}$ rotates in the plane perpendicular to $\hat{\mathbf{z}}$, such that each JP describes a helical trajectory, of radius $R_{\pm} = \sqrt{R_0^2 + a^2 \pm 2aR_0(\mathbf{e}\cdot\hat{\varphi})}$.

Typical trajectories of the two JPs are shown in Fig. 2. Note that the dimer axis $\mathbf{e}$ is constant with respect to the linear motion. In the special case $\mathbf{u}_0 = \mathbf{u}_0'$, the angular velocity vanishes and the dimer moves along a straight line, whereas $\mathbf{u}_0 = -\mathbf{u}_0'$ results in a simple rotation about the center of mass.

III. ADVECTION

A moving particle gives rise to a characteristic velocity field in the surrounding fluid. In addition to its own motion, each particle of a dimer is advected in the velocity field $\mathbf{v}'(\mathbf{r})$ of its neighbor and is also subject to a mechanical force $\mathbf{F}$. Using Faxén's law we find the linear velocity

$$\mathbf{u} = \mathbf{u}_0 + \frac{\mathbf{F}}{\xi} + \mathbf{v}'(-2a\mathbf{e}) + \frac{a^2}{6}\nabla^2\mathbf{v}'(-2a\mathbf{e}), \qquad (8)$$

where $\xi = 6\pi\eta a$ is the usual Stokes friction factor with the viscosity η, and where $\mathbf{v}'$ is evaluated at the distance $\mathbf{R} - \mathbf{R}' = -2a\mathbf{e}$.

For the second particle we find the corresponding expression for $\mathbf{u}'$ by exchanging primed and unprimed quantities,

$$\mathbf{u}' = \mathbf{u}_0' + \frac{\mathbf{F}'}{\xi} + \mathbf{v}(2a\mathbf{e}) + \frac{a^2}{6}\nabla^2\mathbf{v}(2a\mathbf{e}). \qquad (9)$$

Note the change of sign of the argument of the advection flow. For symmetry reasons, the forces cancel each other and are parallel to the dimer axis,

$$\mathbf{F} = F\mathbf{e} = -\mathbf{F}'. \qquad (10)$$

A. Fluid velocity field

Due to some osmotic or catalytic effect, each particle induces an effective slip velocity u_s along its surface. For an axisymmetric Janus particle the slip velocity depends on the polar angle θ only; the leading terms of an expansion in powers of $\cos\theta$ read as

$$u_s(\theta) = \frac{3}{2}u_0 \sin\theta(1 + \beta\cos\theta), \qquad (11)$$

where the factor $\sin\theta$ is characteristic for a sphere [18]. The squirmer parameter β is related to the long-range velocity field $\mathbf{v} \propto \beta r^{-2}$ in the surrounding fluid, and to a large extent determines hydrodynamic interactions with neighbor particles or nearby solid boundaries; an active particle behaves like a "puller" for $\beta > 0$ and like a "pusher" for $\beta < 0$ [19–21]. The higher Fourier components in the expression for $u_s(\theta)$ are of the form $\beta_n dP_n(\cos\theta)/d\theta$ with P_n being the Legendre polynomial of order n; the corresponding velocity field vanishes as $1/r^n$ and $1/r^{(n+2)}$ $(n > 2)$. However, these additional corrections would have little influence on the dimer motion since they would not alter the qualitative picture.

Throughout this paper we assume an axisymmetric slip velocity (11) and we discard any single-particle angular motion. Eq. (11) provides a boundary condition for the velocity field in the surrounding fluid,

$$\begin{aligned}\mathbf{v}_T = &-\frac{1}{2}u_0\frac{a^3}{r^3}(1 - 3\hat{\mathbf{r}}\hat{\mathbf{r}})\cdot\mathbf{n} \\ &-\frac{3}{2}\beta u_0\frac{a^2}{r^2}P_2(\mathbf{n}\cdot\hat{\mathbf{r}})\hat{\mathbf{r}} \\ &+\frac{3}{2}\beta u_0\frac{a^4}{r^4}\Big(P_2(\mathbf{n}\cdot\hat{\mathbf{r}})\hat{\mathbf{r}} - (\mathbf{n}\cdot\hat{\mathbf{r}})(1 - \hat{\mathbf{r}}\hat{\mathbf{r}})\cdot\mathbf{n}\Big), \qquad (12)\end{aligned}$$

where $\hat{\mathbf{r}}$ is the radial unit vector with respect to the particle center, $\mathbf{n}$ is the unit vector along the velocity vector $\mathbf{u}_0$, and P_2 represents the Legendre polynomial of second order [22]. Eq. (12) gives the usual flow field of a self-propelling particle; the first term on the right-hand side occurs for a particle with uniform surface properties in a constant driving field [17], whereas the remainder accounts for the finite squirmer parameter.

In addition to $\mathbf{v}_T$, there is a velocity component arising from the force $\mathbf{F}$,

$$\mathbf{v}_F = \left(\frac{3}{4}\frac{a}{r}(1 + \hat{\mathbf{r}}\hat{\mathbf{r}}) + \frac{1}{4}\frac{a^3}{r^3}(1 - 3\hat{\mathbf{r}}\hat{\mathbf{r}})\right)\cdot\frac{\mathbf{F}}{\xi}. \qquad (13)$$

Note the presence of a long-range Stokeslet contribution proportional to $1/r$. The advection velocity in (9) is given by the sum of the above terms,

$$\mathbf{v} = \mathbf{v}_T + \mathbf{v}_F. \qquad (14)$$

This velocity field is accompanied by the non-uniform pressure

$$P = \frac{\mathbf{F}\cdot\mathbf{r}}{4\pi r^3} - 3\eta\beta u_0\frac{a^2}{r^3}P_2(\mathbf{n}\cdot\hat{\mathbf{r}}), \qquad (15)$$

where the first term is related to the Stokeslet in $\mathbf{v}_F$ and the second one to the r^{-2}-contribution to the squirmer field.

Similar expressions $\mathbf{v}'$ and P' are obtained for the neighbor particle, by replacing the parameters u_0 and $\mathbf{F}$ with corresponding primed quantities.

B. Linear velocity

The center-of-mass velocity of the dimer is given by

$$\mathbf{U} = \frac{\mathbf{u} + \mathbf{u}'}{2}. \qquad (16)$$

Inserting the single-particle velocities (A11) and (A12) we have

$$\begin{aligned}\mathbf{U} = &\left(1 - \frac{\mathbf{Q}}{8}\right)\cdot\mathbf{U}_0 \\ &+\frac{3\beta}{32}\Big(c'\mathbf{u}_0' - c\mathbf{u}_0 + u_0\frac{1 - c^2}{2}\mathbf{e} - u_0'\frac{1 - c'^2}{2}\mathbf{e}\Big), \qquad (17)\end{aligned}$$

where we have defined the quadrupole operator

$$\mathbf{Q} = 1 - 3\mathbf{e}\mathbf{e},$$

and the orientation cosine

$$c = \mathbf{n} \cdot \mathbf{e}, \quad c' = \mathbf{n}' \cdot \mathbf{e}.$$

Note that $\mathbf{U}$ depends on the relative orientation of the particle axes with respect to the dimer axis $\mathbf{e}$.

C. Angular velocity

Similar to Eq. (3), in this case the angular velocity of the dimer with respect to its center is given by

$$\mathbf{\Omega} = \frac{\mathbf{u} - \mathbf{u}'}{2a} \times \mathbf{e}. \tag{18}$$

Inserting the single-particle velocities (A11) and (A12) we find

$$\mathbf{\Omega} = \frac{17}{16}\mathbf{\Omega}_0 + \frac{3\beta}{32a}\Big(c'\mathbf{u}_0' + c\mathbf{u}_0\Big) \times \mathbf{e}. \tag{19}$$

In the first term we have used $\mathbf{Q} \cdot \mathbf{\Omega}_0 = \mathbf{\Omega}_0$, which follows from the fact that $\mathbf{\Omega}_0$ is perpendicular to $\mathbf{e}$. The second term, which is proportional to the squirmer parameter β, results in a correction that is not parallel to $\mathbf{\Omega}_0$.

The angular velocity $\mathbf{\Omega}$ is perpendicular on the dimer axis $\mathbf{e}$. According to the equation of motion

$$\frac{d}{dt}\mathbf{e} = \mathbf{\Omega} \times \mathbf{e}, \tag{20}$$

the dimer axis turns in the plane perpendicular to $\mathbf{\Omega}$ which, as a consequence, is constant in time,

$$\frac{d}{dt}\mathbf{\Omega} = 0. \tag{21}$$

D. Mutual forces

So far the mutual forces (10) are not known; their strength F is determined from the condition that the single-particle velocities have the same component along the dimer axis,

$$(\mathbf{u} - \mathbf{u}') \cdot \mathbf{e} = 0. \tag{22}$$

Inserting the single-particle velocities $\mathbf{u}$ and $\mathbf{u}'$ given in the Appendix and solving for F, we find the force acting on the unprimed particle,

$$\frac{F}{\xi} = \frac{7}{6}(\mathbf{u}_0' - \mathbf{u}_0) \cdot \mathbf{e} - \frac{\beta}{4}\left(u_0 P_2(c) + u_0' P_2(c')\right). \tag{23}$$

IV. DISCUSSION

In the absence of advection, the dimer moves on a helical trajectory (7), as illustrated in Fig. 1. This picture remains valid when including advection corrections, albeit with numerically modified linear and angular velocities $\mathbf{U}$ and $\mathbf{\Omega}$ as expressed by Eqs. (17) and (19).

The helical trajectory is conserved because of the symmetry of the advection field. More complex trajectories would arise if the angular velocity had a component proportional to $\mathbf{e}$, in other words, if the dimer rotated about its axis. Then $\mathbf{\Omega}$ is no longer a constant, resulting in a more intricate motion.

Here we mention two effects that would result in a time dependent angular velocity. First, real Janus particles are not perfectly axisymmetric. In general, their slip velocity comprises a constant in azimuthal direction, resulting in a rotation about the particle axis $\mathbf{n}$ with angular velocity ω_0. Then the angular velocity of the dimer comprises a term proportional to its axis, $\Omega_\parallel = (\omega_0 + \omega_0') \cdot \mathbf{e}$, which leads to a more complex trajectory.

Second, in this paper we have only addressed mutual advection of the two Janus particles, and neglected the influence of their activity. In the case of self-thermophoresis, for example, the slip velocity on the surface of one particle depends not only on its own temperature gradient but also on that of the neighbor,

$$\mathbf{u}_s = \mu(\hat{\mathbf{r}})(\nabla_\parallel T + \nabla_\parallel T'), \tag{24}$$

where $\nabla_\parallel$ is the gradient component parallel to the particle surface. Since in general the mobility μ takes different values on the two hemispheres of a Janus particle, the term $\nabla_\parallel T'$ induces an angular velocity ω_0 about the dimer axis. If the two particles are heated at different temperatures, or show different surface properties, their contributions to $\Omega_\parallel$ do not cancel, and there is a net rotational motion of the dimer about its axis $\mathbf{e}$.

For usual Janus particles these effects are small, and probably could not be distinguished from the rotational diffusion. Thus we are led to the conclusion that advection is the dominant interaction and that dimers in bulk solution move on helical trajectories. One should also keep in mind that gravity can play a role [23]. Because of the heavy metal cap on one hemisphere, the center of mass does not coincide with the geometric center. Then gravity exerts a torque on the dimer, which in particular results in a time-dependent angular frequency vector Ω.

We use the superposition approximation, in other words we neglect higher reflections between the two particles. The reflection method in principle is valid for large distances. But as discussed before, the temperature field is rather insensitive to the presence of a neighbor particle due to a small conductivity difference between the particle and the solvent. On the contrary, the hydrodynamic flow field is sensitive to the presence of the second particle. However, it becomes more important when the particles forming the dimer move with respect to each other. For a rigidly attached dimer, the near-field effects are expected to be less significant. Therefore, a helical like trajectory appears to be a generic feature for such rigid systems. Improving either the superposition approximation by considering higher reflections or con-

sidering higher order terms in Faxén's law would render quantitative changes. But the relatively small linear corrections in Eqs. (17) and (19) (note the prefactor 3/32 in the terms proportional to β) suggest that higher order terms are even smaller and do not change the qualitative picture. Similar numerical changes would result when improving the superposition approximations by applying the method of reflections. Thus, the overall trajectory of a rigid dimer is expected to be close to the helical one unless the additional effects mentioned in the preceding paragraphs are large enough to alter the picture.

We conclude with a remark on the forces (10) exerted by one Janus particle on the other. These mutual forces cancel in the linear and angular velocity, and thus are of little relevance for a rigid dimer. They are important, however, for particles linked by flexible DNA strands, where the length of the macromolecular bridge is determined by equilibrating the entropic force with the mutual force between two JPs, or between a JP and a passive colloid; such hybrid systems have been designed recently [24]. Although, one should keep in mind that for a flexible coupling, the two particles also exert torques on each other which results in a more complex rotation than that of a rigid dimer.

Acknowledgments

Stimulating discussions with Alois Würger are gratefully acknowledged.

Author contribution statement

A. M. conceived the problem, performed all the calculations, and wrote the manuscript.

Appendix A: Single-particle velocities

Here we give the advection corrections to the velocities $\mathbf{u}$ and $\mathbf{u}'$ of the Janus particles forming the dimer. We evaluate the different contributions to the right hand sides of Eqs. (8) and (9).

We start with the velocity field $\mathbf{v}$ created by the unprimed particle at the position of its neighbor (i.e., $\mathbf{r} = 2a\mathbf{e}$). There are two contributions, $\mathbf{v}(2a\mathbf{e}) = \mathbf{v}_T(2a\mathbf{e}) + \mathbf{v}_F(2a\mathbf{e})$, which arise from the particle's self-propulsion and the force exerted by its neighbor, respectively. From the explicit expressions given in Eqs. (12) and (13), one readily obtains the advection terms

$$\mathbf{v}_T(2a\mathbf{e}) = -\frac{3}{8}\beta u_0 P_2(c)\mathbf{e} - \frac{\mathbf{Q}\cdot\mathbf{u}_0}{16} + \frac{3\beta u_0}{32}\left[P_2(c)\mathbf{e} - c(1-\mathbf{ee})\cdot\mathbf{n}\right], \quad \text{(A1)}$$

and

$$\mathbf{v}_F(2a\mathbf{e}) = \left(\frac{3\,(1+\mathbf{ee})}{8} + \frac{\mathbf{Q}}{32}\right)\cdot\frac{\mathbf{F}}{\xi}. \quad \text{(A2)}$$

The correction term is evaluated by using Stokes' equation $\eta\nabla^2\mathbf{v} = \nabla P$ with the expression for the pressure given in Eq. (15). Thus we find the contribution arising from self-propulsion,

$$\nabla^2\mathbf{v}_T = 9\beta u_0\frac{a^2}{r^4}\Big(P_2(\mathbf{n}\cdot\hat{\mathbf{r}})\hat{\mathbf{r}} - (\mathbf{n}\cdot\hat{\mathbf{r}})(1-\hat{\mathbf{r}}\hat{\mathbf{r}})\cdot\mathbf{n}\Big), \quad \text{(A3)}$$

and similarly that due to the mutual force,

$$\nabla^2\mathbf{v}_F = (1-3\hat{\mathbf{r}}\hat{\mathbf{r}})\cdot\frac{\mathbf{F}}{4\pi\eta r^3}. \quad \text{(A4)}$$

Putting $\mathbf{r} = 2a\mathbf{e}$ and using the definitions for c and $\mathbf{Q}$, we have

$$\frac{a^2}{6}\nabla^2\mathbf{v}_T(2a\mathbf{e}) = \frac{3\beta u_0}{32}\Big(P_2(c)\mathbf{e} - c(1-\mathbf{ee})\cdot\mathbf{n}\Big), \quad \text{(A5)}$$

and

$$\frac{a^2}{6}\nabla^2\mathbf{v}_F(2a\mathbf{e}) = \frac{\mathbf{Q}\cdot\mathbf{F}}{32\xi}. \quad \text{(A6)}$$

We give the corresponding quantities for the primed particle at the relative position $\mathbf{r} = -2a\mathbf{e}$ (note that the unit vector $\mathbf{e}$ points from the unprimed to the primed particle):

$$\mathbf{v'}_T(-2a\mathbf{e}) = \frac{3}{8}\beta u'_0 P_2(c')\mathbf{e} - \frac{\mathbf{Q}\cdot\mathbf{u'}_0}{16} + \frac{3\beta u_0}{32}\left[-P_2(c')\mathbf{e} + c'(1-\mathbf{ee})\cdot\mathbf{n}'\right], \quad \text{(A7)}$$

$$\mathbf{v'}_F(-2a\mathbf{e}) = \left(\frac{3\,(1+\mathbf{ee})}{8} + \frac{\mathbf{Q}}{32}\right)\cdot\frac{\mathbf{F}'}{\xi}, \quad \text{(A8)}$$

$$\frac{a^2}{6}\nabla^2\mathbf{v'}_T(-2a\mathbf{e}) = \frac{3\beta u'_0}{32}\Big(-P_2(c')\mathbf{e} + c'(1-\mathbf{ee})\cdot\mathbf{n}'\Big), \quad \text{(A9)}$$

and,

$$\frac{a^2}{6}\nabla^2\mathbf{v'}_F(-2a\mathbf{e}) = \frac{\mathbf{Q}\cdot\mathbf{F}'}{32\xi}. \quad \text{(A10)}$$

Finally, inserting Eqs. (A1-A10) in (8) and (9), one obtains the single-particle velocities

$$\mathbf{u} = \mathbf{u}_0 - \frac{\mathbf{Q}\cdot\mathbf{u'}_0}{16} + \frac{\mathbf{F}}{\xi} + \frac{5}{8}\frac{\mathbf{F}'}{\xi} + \frac{3\beta}{16}\Big(u'_0 P_2(c')\mathbf{e} + c'(1-\mathbf{ee})\cdot\mathbf{u'}_0\Big), \quad \text{(A11)}$$

and

$$\mathbf{u}' = \mathbf{u'}_0 - \frac{\mathbf{Q}\cdot\mathbf{u}_0}{16} + \frac{\mathbf{F}'}{\xi} + \frac{5}{8}\frac{\mathbf{F}}{\xi} - \frac{3\beta}{16}\Big(u_0 P_2(c)\mathbf{e} + c(1-\mathbf{ee})\cdot\mathbf{u}_0\Big). \quad \text{(A12)}$$

Using $\mathbf{F}' = -\mathbf{F}$ further simplifies the force terms.

[1] S. J. Ebbens and J. R. Howse, Soft Matter **6**, 726 (2010).
[2] M. E. Cates, Rep. Prog. Phys. **75**, 042601 (2012).
[3] R. Dreyfus, J. Baudry, M. L. Roper, M. Fermigier, H. A. Stone, and J. Bibette, Nature **437**, 862 (2005).
[4] J. Elgeti, R.G. Winkler, and G. Gompper, Rep. Prog. Phys. **78**, 056601 (2015).
[5] S. Sundararajan, P. E. Lammert, A. W. Zudans, V. H. Crespi, and A. Sen, Nano Lett. **8**, 1271 (2008).
[6] R. Laocharoensuk, J. Burdick, and J. Wang, ACS Nano **2**, 1069 (2008).
[7] W. F. Paxton, K. C. Kistler, C. C. Olmeda, A. Sen, S. K. St. Angelo, Y. Cao, T. E. Mallouk, P. E. Lammert, and V. H. Crespi, J. Am. Chem. Soc. **126**, 13424 (2004).
[8] W. F. Paxton, P. T. Baker, T. R. Kline, Y. Wang, T. E. Mallouk, and A. Sen, J. Am. Chem. Soc. **128**, 14881 (2006).
[9] J. R. Howse, R. A. L. Jones, A. J. Ryan, T. Gough, R. Vafabakhsh, and R. Golestanian, Phys. Rev. Lett. **99**, 048102 (2007).
[10] R. Golestanian, T. B. Liverpool, and A. Ajdari, Phys. Rev. Lett. **94**, 220801 (2005).
[11] H.-R. Jiang, N. Yoshinaga, and M. Sano, Phys. Rev. Lett. **105**, 268302 (2010).
[12] A. P. Bergulla and F. Cichos, Faraday Discuss. **184**, 381 (2015).
[13] L. Baraban, R. Streubel, D. Makarov, L. Han, D. Karnaushenko, O. G. Schmidt, and G. Cuniberti, ACS Nano **7**, 1360 (2013).
[14] F. Kümmel, B. ten Hagen, R. Wittkowski, I. Buttinoni, R. Eichhorn, G. Volpe, H. Löwen, and C. Bechinger, Phys. Rev. Lett. **110**, 198302 (2013).
[15] A. Wittmeier, A. L. Holterhoff, J. Johnson, and J. G. Gibbs, Langmuir **31**, 10402 (2015).
[16] N. S.-Mood, A. Mozaffari, and U. M. C.-Figueroa, J. Fluid Mech. **798**, 910 (2016).
[17] J.L. Anderson, Ann. Rev. Fluid Mech. **21**, 61 (1989).
[18] J. R. Blake, J. Fluid Mech. **46**, 199 (1971).
[19] T. Ishikawa, M. P. Simmonds, and T. J. Pedley, J. Fluid Mech. **568**, 119 (2006).
[20] I. Llopis and I. Pagonabarraga, J. Non-Newtonian Fluid Mech. **165**, 946 (2010).
[21] A. Zöttl and H. Stark, Phys. Rev. Lett. **112**, 118101 (2014).
[22] T. Bickel, A. Majee, and A. Würger, Phys. Rev. E **88**, 012301 (2013).
[23] A. I. Campbell and S. J. Ebbens, Langmuir **29**, 14066 (2013).
[24] R. Schachoff, M. Selmke, A. Bregulla, F. Cichos, D. Rings, D. Chakraborty, K. Kroy, K. Günther, A. Henning-Knechtel, E. Sperling, M. Mertig, diffusion-fundamentals.org **23**, 1 (2015).